Generation of Gradient Index Optics with Subwavelength Metamaterials

A THESIS SUBMITTED TO THE FACULTY OF THE GRADUATE SCHOOL OF THE UNIVERSITY OF MINNESOTA BY

Andrew Steven Borowiak

IN PARTIAL FULFILLMENT OF THE REQUIREMENTS FOR THE DEGREE OF MASTER OF SCIENCE

JAMES R. LEGER, ADVISOR

July 2019

Acknowledgements

I would first like to thank Erik Tilsith, without whom I would not have found myself in this research group. He casually suggested I talk to Professor Leger about something he was working on, and it turned into my thesis project.

I also want to thank Mint Kunkel for answering the many questions I have had for the past two years. Mint has been a fantastic resource and an abundant source of information throughout the project. He spent multiple hours helping me find potential solutions to problems I was encountering. It is thanks to his research that this GRIN design process exists in the first place. He also provided all the GRIN mode converter index profiles used in my design process. I would not have finished this project at the rate that I did without him.

Finally, I would like to thank Professor James Leger, who often inspired me to go the extra step with my simulations, so much so that I often went too many steps ahead and lost confidence in my designs, but he was always there to help me see how to step back and regain my confidence. And of course, I could not have done this project if he had not asked me to join his research group!

Abstract

A GRIN optic is a useful device for modern optics but is not frequently used outside of niche applications due to the difficulty of fabricating any arbitrary gradient index. One potential solution to this fabrication problem is to use subwavelength metamaterials generated using lithography. A process was developed to generate a subwavelength waveguide which leverages effective medium theory to behave like a GRIN optic. This process was tested by generating waveguides as well as mode converters for converting from gaussian beams to supergaussian beams. The results from these experiments show that this technique could produce mode converters with average Strehl ratios of 0.997 and an average transmission of 94.8% on the scale of tens of microns; however, it was found that these designs are not viable for modern lithographic fabrication techniques. There is much to explore still with this topic such as the lower size limits of these designs or whether modern lithography could make a mode converter with this structure.

Table of Contents

List of Figures

Introduction

A Gradient Refractive Index (GRIN) optical device is a device in which the index of refraction is a function of spatial positions (x, y, z). GRIN devices with continuous profiles have been used in niche applications where parabolic profiles are useful, such as in fiber optics, for many years, but recent advancements in fabrication technology have made it viable to produce discrete index profiles, which are able to have arbitrary index profiles.

If the index profile of a GRIN device is known, the output beam profile, given any input beam profile, can be predicted. This problem can be solved in reverse for an index profile given an input and output beam profile. In theory, this can be used to convert from one beam profile to another with zero loss. For example, a GRIN can be made as an optical mode converter used to convert from a gaussian beam to a flat-top beam. This allows for highly efficient mode-matching for coupling between different optical devices. Other examples where a GRIN optic might be useful is in coherent beam combining, medical devices, and beam splitting.

GRIN devices are widely used in communication systems. These GRIN devices were fabricated with a parabolic index profile to maintain a gaussian beam. Parabolic index profiles are one type of index profile which are relatively easy to produce. This ease of production caused them to be used extensively for a few niche applications such as in fiber optic communication systems or in compact copiers. Most other GRIN profiles are difficult to produce with conventional methods and thus GRIN devices have not been used frequently in other areas of optics.

The purpose of this project was to test whether an arbitrary 2D GRIN profile could be fabricated using a set of subwavelength lens-like structures to form a waveguide with a GRIN profile. The end goal of this project was to determine if lithography was a viable way to fabricate one of the lens train structures.

This thesis first gives some background needed to understand the research performed. Next, the generation of a continuous GRIN block is discussed. In this section, the index profiles required to maintain a gaussian beam profile as well as a supergaussian beam profile are predicted. These continuous GRIN blocks are then tested to prove their effectiveness as waveguides. These findings are then extended from the continuous GRIN block to a subwavelength waveguide GRIN device. The performances of these structures are evaluated, as well as their ability to be fabricated using lithography. A geometry that may improve fabrication results is briefly discussed. These structures are tested and compared to their continuous counterparts. Next, the generation of a mode converter GRIN optic using subwavelength structures is introduced. The performance of these designs is discussed, and points of further research are listed. Finally, a conclusion is reached, and points of further research are discussed.

Appendices have also been included that discuss implementation of these devices using the FDTD simulation environment called Lumerical. The details of how Lumerical functions are discussed and suggestions are given for those that would look to implement a similar system. This section is intended to complement the rest of the paper and is not needed for the typical reader.

Background Information

GRIN devices have many potential uses but are not pervasive in modern optics. This is largely due to the difficulties associated with fabricating a device which continually varies in index. There are few methods that are able to generate truly continuous GRIN devices. An example of one such method is ion exchange, which was one of the most widely used methods of GRIN fabrication in the 1980s. In the ion exchange method, a material is submerged in a salt bath, where the ions of the salt diffuse into the optic [1]. This allows for the generation of parabolic GRIN profiles. Since this method limits which profiles can be made, and the process for making GRIN devices in this manner is relatively slow, it is a non-ideal method of fabrication in most cases. Another method of generating a truly continuous GRIN is to pull crystals of material from vats of doped liquid, which gives rise to a gradient index in the pull direction as the relative concentration of the impurities increases in the vat of molten material [1]. This method does not scale well, and can be relatively costly, making it non-ideal for most cases.

Continuous profiles have been used successfully for many years, however the lack of methods to fabricate non-parabolic GRIN devices makes them unfavorable in most applications. This has led to the development of methods to make continuous-like gradients from discrete elements. There are now many ways to create discrete GRIN profiles which behave similarly to continuous GRIN devices. These methods of fabrication tend to be relatively fast compared to continuous GRIN fabrication methods, can make smaller devices, and allow for much more freedom in GRIN profile design.

One of the fundamental principles of wave physics is that when a wave hits a medium discontinuity, some of the wave power is reflected. This property carries into optics, where the wave is an electromagnetic wave, and the medium is represented by the index of refraction. This property is often described with the Fresnel equations and called Fresnel reflection. When the index discontinuities are separated by a period P, and the wave has wavelength 2P/N, where N is an integer, then all the power from the wave will be reflected in an infinitely long device. This is because the reflected waves from each discontinuity interfere constructively. This property is used to reflect specific wavelengths of light in devices called Bragg filters.

If the index discontinuities have a period less than half a wavelength then the structure still causes Fresnel reflection, as it would with periodicity larger than half a wavelength; but when the periodicity is this small, waves begin behaving as though they are passing through a continuous medium, this is called effective medium theory. Effective medium theory states that on small size scales relative to the wavelength, the discontinuous medium behaves like a single continuous material. This is because the Fresnel reflections from each discontinuity interfere destructively, forcing the power of the Fresnel reflection to zero. For effective medium theory-based solutions, the polarization of the light used in the system must be known, as different polarizations of light will experience a different effective medium. The equations for the effective index of a periodic discontinuous medium made of two materials for a TE wave and a TM wave are

$$TE\colon\ n_{eff}^2(y) = \frac{n_1^2 f(y)}{P} + \frac{n_2^2\big(P - f(y)\big)}{P}$$

$$TM\colon\ n_{eff}^{-2} = \frac{n_1^{-2} f}{P} + \frac{n_2^{-2}(P-f)}{P}$$

where P is the periodicity of the subwavelength structure, n_1 is the index of refraction of medium 1, n_2 is the index of refraction for medium 2, and f is the amount of material 1 in each period P [2]. For a TE wave, the effective index profile in a discontinuous medium, assuming non-magnetic materials, is the square root of the local geometric average of the permittivity. This behavior gives discontinuous GRIN devices the ability to function as a metamaterial and can be leveraged to design subwavelength structures. A metamaterial is a device made of subwavelength components. Metamaterials are designed to behave like a single material with a property that is typically difficult to find naturally, such as having a GRIN profile. The square root of the local average of the permittivity profile gives a continuous index profile.

There are currently many methods to make subwavelength metamaterial-based GRIN devices. One such method is chemical vapor deposition. In this method, layers of material are deposited onto a surface, and a GRIN is obtained by varying the index of the deposited material, and continuous-like structures are made when the layers are thin with respect to the wavelength [1]. This method allows for the creation of GRIN profiles that vary in one dimension. Another option to generate subwavelength GRIN profiles to use femtosecond laser writing, where the index of a material is locally changed through exposure with a laser, where the index change is proportional to the pulse energy [3]. This process allows for complete control of the GRIN profile in two dimensions, but little to no control in the third dimension. These are only a few methods which allow for

subwavelength metamaterial-based GRIN design; however most share a common issue, fabricating very small devices with these techniques is difficult.

A method for fabricating very small subwavelength metamaterial-based GRIN devices is by use of lithography. In lithography, structures which are small enough to be averaged by effective medium theory are generated through several different methods. One method is to etch away material after having applied a mask [4]. This allows for the creation of 2D GRIN devices by generating structures that give the desired effective index. Another option which allows for the generation of 3D structures is liquid deposition photolithography, wherein patterns are cured into layers of material. After curing, time is given for the diffusion of the remaining liquid sections into the cured sections to increase the index of the cured section, then the whole layer is cured and lowered, allowing another liquid layer to be patterned on top [5].

GRIN devices are useful because they can, in theory, have any index profile and perform any arbitrary optical function. This raises the question of how to design an index profile for a given application. If diffraction effects are negligible, then a 2D GRIN device can be designed using ray optics. A process for generating a 2D GRIN profile with this method is as follows [6]. First, the desired input and output beam intensity and phase profiles should be determined. From this information, the input and output profiles should be converted into rays, wherein the linear density of the rays is an indicator of the power distribution in the profile, and the direction of the ray is an indicator of the desired relative phase for that linear position. The same number of rays should be used for both the input profile and output profile, as the next step involves connecting input rays to output rays. The rays should be specified such that the linking lines do not intersect, and

the input/output ray angle matches the angle of the linking lines at the input/output. These linking lines must be continuous, have continuous second partial derivative in the propagation direction, have continuous second mixed partial derivatives, and have continuous, non-zero, mixed first derivatives. There is not currently any optimal shape for the linking lines, though both sinusoids and third order polynomials have been used successfully. This process gives the direction of power flow at all locations within the GRIN, from which the relative phase of the propagating beam can be interpreted for each point, as the lines of constant phase should always be perpendicular to the direction of power propagation. From the relative phase profile, the GRIN profile can be found through the Eikonal equation.

This method was extended further to include situations wherein diffraction is non-negligible [7]. This method uses a split step beam propagation method to account for the effects of diffraction. Split step beam propagation, combined with phase retrieval, produces a GRIN profile that corrects the effect of diffraction in each step.

These methods of generating arbitrary 2D GRIN profiles have been shown to work well in theory, but fabrication has been problematic. One example where a 2D GRIN mode converter was designed and fabricated can be found in work done previously by our group, where a modified femtosecond laser writing technique was used to generate a 2D mode converter [3]. The fabricated device was unable to successfully perform exactly as intended, as the fabrication process distorted the index profile causing the converter to work sub optimally. This process could in theory be used to fabricate 2D GRIN devices, but the fabrication time for a device using this method is relatively long.

The goal of this research was to locate a fabrication domain in which these devices have potential to be fabricated quickly, cheaply, easily, and with precision. Inspired by recent studies of subwavelength waveguides, lithography was considered as a method for fabricating a GRIN device. Modern lithographic etching techniques using electron beams can fabricate objects with an accuracy of 50nm [2]. Compared to other methods of generating GRIN structures, lithography is also fast and inexpensive. It was decided that the goal of further research would be to explore the generation of GRIN devices using subwavelength silicon structures, leveraging effective medium theory to generate 2D GRIN devices.

Using effective medium theory and lithographic etching techniques has been explored previously. Subwavelength rectangular prisms can be etched into silicon, as is shown in Figure 1, to form what is effectively a ridge waveguide [8].

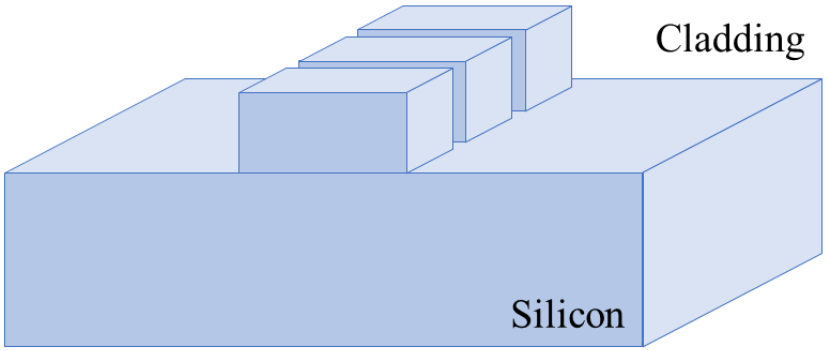

Figure 1: An example of a subwavelength waveguide etched in silicon. In this geometry the waveguide behaves similarly to a ridge waveguide made of three separate materials.

The subwavelength rectangular prisms in this structure are small enough to make the structure behave like an effective medium. This means that the line of prisms appears to be a single medium with uniform refractive index. These structures appear to be made of three materials: the cladding material, silicon, and a third material with an index value

between that of the cladding material and silicon. Simple GRIN devices have been fabricated in this domain with multiple different structures as well. As an example, parabolic GRIN designs have been fabricated using a subwavelength pulse width modulation scheme in the transverse direction of the waveguide [9]. This structure used subwavelength blocks with varying duty cycle in the transverse direction to simulate a 1D GRIN structure which had a parabolic index profile with the effective medium theory approximation. This method of forming a GRIN device is effective for the 1D case, as there are no Bragg resonances in the device because the subwavelength gratings are not in the direction of propagation. Another way that lithography is used in conjunction with effective index theory is in photonic crystals used in transformation optics [10]. These structures use subwavelength GRIN optics to bend the light around the structure, making it invisible to specific frequencies of light.

The Strehl ratio was used for all tests as a way of quantifying the quality of all the GRIN structures designed in this thesis. The Strehl ratio was used as a metric to compare the similarity between the experimental beam outputs and the expected output beam. The Strehl ratio should always take a real value between 0 and 1. A ratio of 1 implies that the electric field of the experimental output beam is identical, or nearly identical to the ideal output beam. For electric fields E and Ψ, the Strehl ratio is defined as

$$Strehl\ Ratio = \frac{|\iint E\Psi^* \, dxdy|^2}{(\iint |E|^2 \, dxdy)(\iint |\Psi|^2 \, dxdy)}$$

where "*" denotes the complex conjugate.

Continuous GRIN Guides

Gaussian Guide

To showcase that the subwavelength GRIN structures would behave as expected, a benchmark test was needed for comparison. The goal with using subwavelength GRIN structures was to imitate a continuous GRIN structure, so the best way to test these structures was to first test how the continuous versions of these structures behaved.

The fundamental mode of a waveguide is the electric field magnitude and phase profile that will propagate through the waveguide without varying. This problem can be solved in reverse for the index profile needed to maintain a given beam profile. The index profile needed to maintain the shape of an input gaussian beam is of the form

$$n^2(y) = n_o^2(1 - (gy)^2)$$

where n_o is the background index of the material, g is the curvature of the parabola, and y is the distance from the beam center. The beam propagates along the x axis, and the z axis is considered infinite and uniform for both the beam and the GRIN block [11]. The ABCD matrix for a continuous GRIN block with this parabolic index profile is given as

$$\begin{bmatrix} \cos(gl) & \frac{\sin(gl)}{g} \\ -gsin(gl) & \cos(gl) \end{bmatrix}$$

where l is the propagation length. Since the input to the GRIN block is a gaussian beam, the ABCD Law for gaussian beams can be used, which states that

$$q_{out} = \frac{Aq_{in} + B}{Cq_{in} + D}$$

where q_{in} is the input complex curvature of the gaussian beam and q_{out} is the output gaussian beam's complex curvature [11]. Substituting in the ABCD matrix for this equation gives

$$q_{out} = \frac{\cos(gl)\, q_{in} + \sin(gl)/g}{\cos(gl) - g\sin(gl) q_{in}}.$$

Since the input beam should be identical to the output beam, no matter what length block chosen, q_{out} can be set equal to q_{in} and this equation can be solved to find that

$$\frac{1}{q_{out}} = \frac{1}{q_{in}} = ig.$$

The complex curvature of a gaussian beam is defined as

$$\frac{1}{q_{in}} = \frac{1}{R(x)} + \frac{-i\lambda_o}{\pi w^2(x) n},$$

where R(x) is the radius of curvature of the phase front, which is infinite at x=0; $i = \sqrt{-1}$ λ_o is the free space wavelength of the beam; $w(x)=w_o$ at x=0; and n is approximated to the background index n_o [11]. The point x=0 is called the beam waist and it is the point on a gaussian beam which has a flat phase front and the smallest spatial distribution of light. It is assumed that the beam waist will be at the front surface of the GRIN device. From this information, it can be shown that

$$g = \frac{-\lambda_o}{\pi w_o^2 n_o}.$$

Note that the negative sign on g does not affect the curvature of the parabola, as g^2 is the curvature. Substituting this result into the index equation, the index profile needed to

confine and maintain an input gaussian beam of wavelength λ_o and beam waist w_o is found to be

$$n(y) = \sqrt{n_o^2 - \frac{\lambda_o^2 y^2}{\pi^2 w_o^4}}$$

where n_o is the background index of the material, the beam waist is in or at the front face of the GRIN block, and the beam propagates along the x axis.

To show that this was in fact the correct index profile to maintain a gaussian beam, a simulation was performed where gaussian beams of different beam waists were propagated through a continuous GRIN block designed to maintain a 4 μm gaussian beam of 1.5 μm light with a background index of 1.5. These tests were able to show that the parabolic index was able to maintain the gaussian beam it was designed for, while gaussian beams with different beam waists were not properly maintained. The 4 μm input beam had a Strehl ratio of 1, the 2 μm input beam had a Strehl ratio of 0.647, and the 8 μm input beam had a Strehl ratio of 0.6431.

The results of these tests can be seen in Figure 2. Note that the GRIN was designed for a 4 μm beam, and the output profiles shown are for input gaussian beams with waists of 2 μm, 4 μm, and 8 μm from left to right respectively. These output beams are still gaussian beams but have not maintained the profile that was used at the input of the device. Since these parabolic GRIN devices were found to work well, more complicated GRIN devices were designed to maintain a supergaussian beam profile.

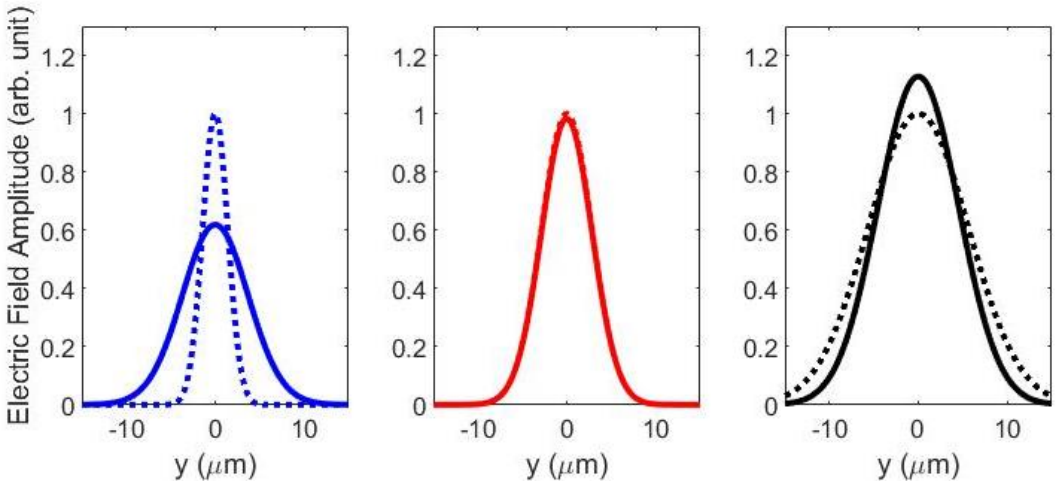

Figure 2: The output electric field magnitude profiles generated by propagating a gaussian through a GRIN designed to maintain a gaussian with a beam waist of 4 μm. From left to right, the inputs to the GRIN are a 2 μm beam, a 4 μm beam, and an 8 μm beam. The dashed lines are the input beam profiles and the solid lines are the output profiles.

Supergaussian Guide

We next wanted to design a continuous GRIN waveguide for a flat top beam profile. A flat top beam profile is a beam which has a uniform magnitude profile to a certain distance, at which point the magnitude drops to zero. The flat top beam is often approximated by a supergaussian of order 10. A supergaussian has an E field magnitude profile of the form

$$E(y) = Ae^{-\left(\frac{y}{W}\right)^M}$$

where A is a field scaling factor, y is the distance from the center of the beam, W is known as the beam waist, and M is the order of the beam. Notice that if M=2, this is the equation for a gaussian. Figure 3 shows an example of a supergaussian with M=10, W=1, and A=1 as well as an example of a similar flat top.

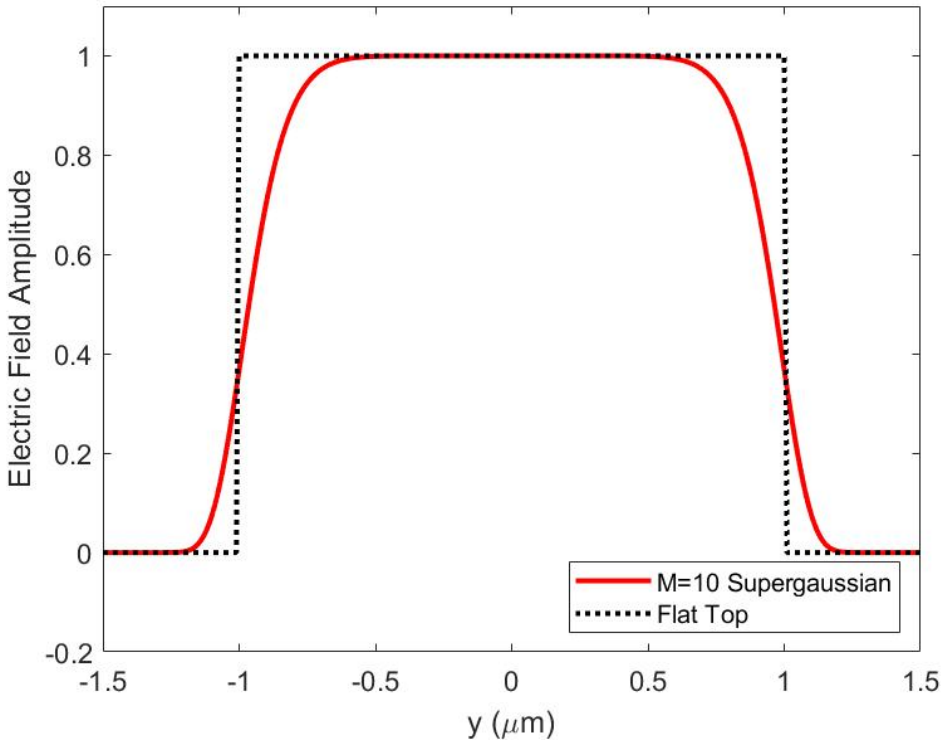

Figure 3: Shows a comparison between the electric field profiles of an ideal flat top beam and a 10^{th} order supergaussian, both have maximum field amplitude of 1 and beam waist of 1.

The continuous GRIN profile can be calculated using the paraxial propagation equation,

$$\frac{d^2E(y)}{dy^2} + 2k^2\Delta n(y)E(y) = 0.$$

Note that to use this equation, the index profile must not vary with propagation direction x or with the other transverse direction z, and the field is assumed to not change with propagation [12]. E(y) is the field of the beam and Δn(y) is defined by

$$n(y) = n_o\big(1 + \Delta n(y)\big),$$

where n_o is the background index and n(y) is the desired index profile. The variable k is the wavenumber which is defined as

$$k = \frac{2\pi n_o}{\lambda_o}.$$

For all tests performed, the background index n_o is set to 1.5. Solving this system of equations yields that

$$n(y) = n_o\left(1 + \frac{M(M-1)y^{M-2}\lambda_o^2}{8\pi^2 W^M n_o^2} - \frac{M^2 y^{2M-2}\lambda_o^2}{8\pi^2 W^{2M} n_o^2}\right).$$

Using values of M=10, W=5 μm, n_o=1.5, and λ_o=1.5, one ends up with the index profile shown in Figure 4.

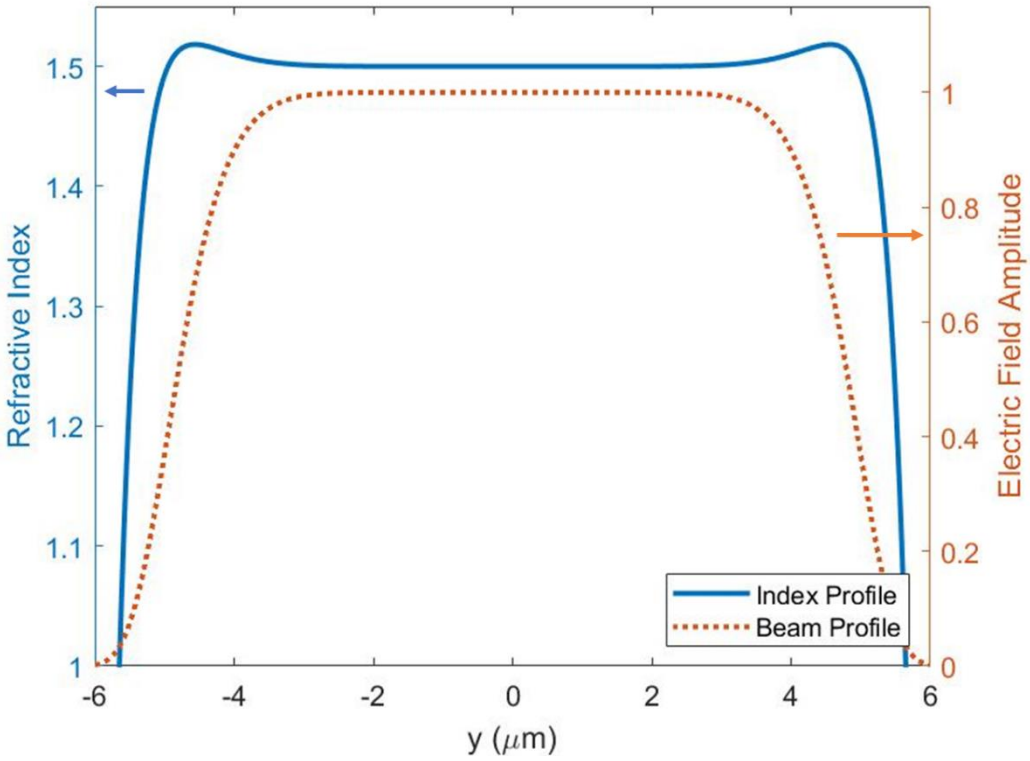

Figure 4: Shows the Bat Ears index profile required to maintain a 1.5 μm 10th order supergaussian beam with a beam waist of 5 μm and a background index of 1.5. The shape of the design beam is shown for reference.

This profile has been named a "Bat Ears profile" due to its Batman-like shape. To test the validity of the many approximations used to obtain this solution, this equation

was used to design for a gaussian beam, also known as a supergaussian beam of order M=2, which leads to the equation

$$n(y) = n_o\left(1 + \frac{\lambda_0^2}{4\pi^2 W^2 n_o^2} - \frac{y^2\lambda_o^2}{2\pi^2 W^4 n_o^2}\right).$$

This equation is easily comparable to the parabolic index profile equation outlined previously as

$$\sqrt{n_o^2(1 - g^2y^2)} = n(y) = n_o\sqrt{1 - g^2y^2}.$$

This equation can be approximated using the binomial approximation to be

$$n(y) \approx n_o\left(1 - \frac{g^2y^2}{2}\right).$$

This shows that the binomial approximation of the parabolic equation is nearly identical to the equation derived through the paraxial propagation equation. The only difference between these equations is the slight background index shift created by the center term in the Helmholtz derived equation. This difference is a result of the many approximations used in these equations such as the paraxial approximation, the binomial approximation, and the scalar wave approximation. The paraxial approximation, for example, allows for the background index to shift without affecting the fundamental mode shape.

To prove that the Bat Ears equation would guide a supergaussian correctly, a continuous GRIN block with an index profile designed for a 10 μm supergaussian beam of 1.5 μm light and a background index of 1.5 was simulated using Lumerical. Lumerical predicted that this structure would guide the supergaussian it was designed for nearly perfectly while supergaussians of different sizes were unable to propagate without their

field profiles changing. The results of this test are shown in Figure 5. The Strehl ratio for the 9 μm input beam was 0.9618, the Strehl ratio for the 10 μm beam was 1, and the Strehl ratio for the 11 μm beam was 0.9576. This design worked very well, maintaining a Strehl ratio of 1. Next, the discontinuous GRIN profile design process is researched.

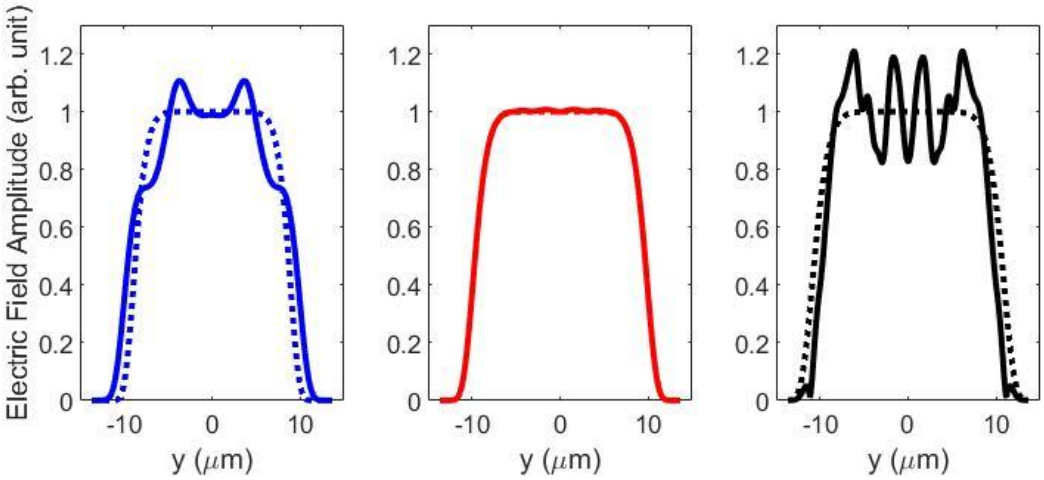

Figure 5: The output electric field magnitude profiles generated by propagating a 10th order supergaussian through a GRIN designed to maintain a 10th order supergaussian with a beam waist of 10 μm. From left to right, the inputs to the GRIN are a 9 μm beam, a 10 μm beam, and an 11 μm beam. The dashed lines are the input beam profiles and the solid lines are the output profiles.

Subwavelength GRIN Guides

Parabolic Lens Train

The next goal was to build and test the first subwavelength GRIN structure. The goal was to make a parabolic GRIN using a train of lenses with a uniform refractive index. The subwavelength structures were lens shaped to generate the parabolic effective index profile. The lens train was designed as shown in Figure 6.

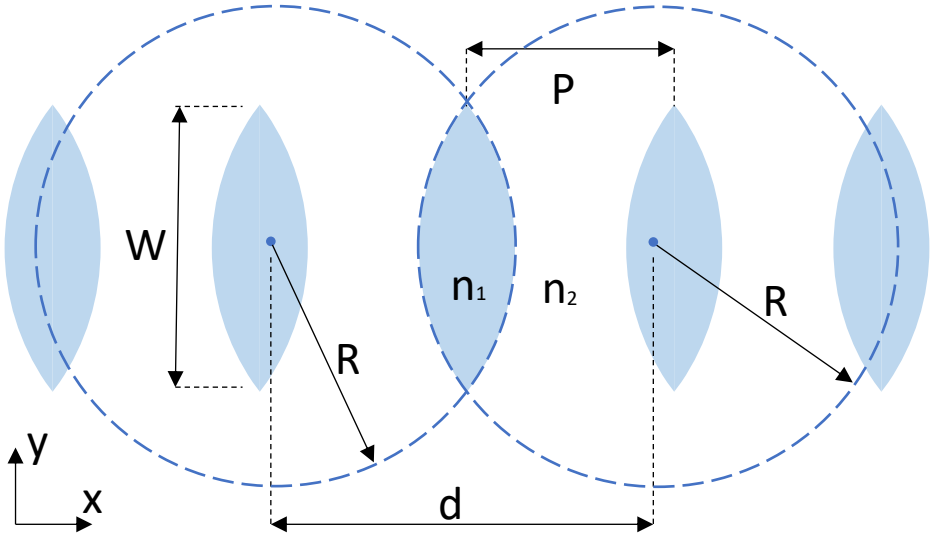

Figure 6: The design parameters for a subwavelength lens train. P is the lens period, W is the transverse width of the lens, R is the radius of curvature of the lens face, d is the distance between the centers of the circles which form the lens. The lens material has refractive index n_1 and the cladding material has refractive index n_2.

In this lens train, P represents the lens period, R represents the radius of the lens faces, d is the distance between the centers of curvature for each face of the lens, W is the transverse width of the lenses, n_1 is the index of the lenses, and n_2 is the index of the cladding, which is the material surrounding the lenses. This geometry was converted into equations by observing that the lens thickness at any point along y is

$$f(y) = 2\sqrt{R^2 - \left(\frac{y}{2}\right)^2} - d.$$

The variable d can be eliminated by knowing that

$$d = 2\sqrt{R^2 - \left(\frac{W}{2}\right)^2}.$$

From effective medium theory, the effective index of refraction for a TE mode is

$$n_{eff}^2(y) = \frac{n_1^2 f(y)}{P} + \frac{n_2^2(P - f(y))}{P},$$

where P is the periodicity of the subwavelength structure, n_1 is the index of refraction of medium 1, n_2 is the index of refraction for medium 2, and f is the amount of material 1 in each period P [2]. Substituting these equations together, the resulting equation is

$$n_{eff}^2(y) = \frac{n_1^2\left(2\sqrt{R^2 - \left(\frac{y}{2}\right)^2} - 2\sqrt{R^2 - \left(\frac{W}{2}\right)^2}\right)}{P} + \frac{n_2^2\left(P - 2\sqrt{R^2 - \left(\frac{y}{2}\right)^2} - 2\sqrt{R^2 - \left(\frac{W}{2}\right)^2}\right)}{P}.$$

Using these equations, the parameters to make a lens train designed for a 4 μm beam are found, for more information, see Appendix 1. This lens train was tested with a few gaussians of different beam waists and it was found that Parabolic lens train maintained a 4 μm beam but was unable to maintain 2 μm or an 8 μm beam, showing that this structure is behaving like a continuous GRIN structure. These results are shown in Figure 7. The Strehl ratio for the 2 μm beam was 0.6953, the Strehl ratio for the 4 μm beam was 1, and the Strehl ratio for the 8 μm beam was 0.7014.

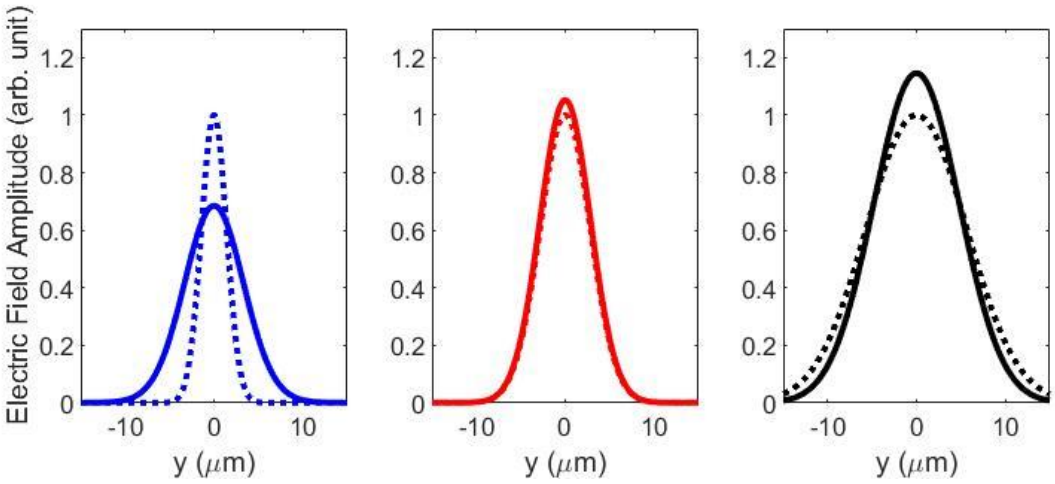

Figure 7: The output electric field magnitude profiles generated by propagating a gaussian through a GRIN designed to maintain a gaussian with a beam waist of 4 μm. From left to right, the inputs to the GRIN are a 2 μm beam, a 4 μm beam, and an 8 μm beam. The dashed lines are the input beam profiles and the solid lines are the output profiles.

This structure was also tested with a larger lens periodicity, one where the period between lens was large enough to make this structure behave like a Bragg reflector. It was found that this structure did in fact behave like a Bragg reflector, as a large portion of the input beam was reflected out the front of the Lens train, and only a small percentage reached the back end of the Lens train.

Bat Ears Lens Train

Once the Parabolic lens train was tested, the process for converting the Bat Ears continuous index profile into a lens train was considered. Here, a similar methodology as had used in the design of a Parabolic lens train was used to generate the Bat Ears lens train. Given the equation

$$n(y) = n_o\left(1 + \frac{M(M-1)y^{M-2}\lambda_o^2}{8\pi^2 W^M n_o^2} - \frac{M^2 y^{2M-2}\lambda_o^2}{8\pi^2 W^{2M} n_o^2}\right),$$

the effective index equation for a TE wave can be used to solve for the geometry of the lenses

$$n^2(y) = \frac{n_1^2 f(y)}{P} + \frac{n_2^2 (S - f(y))}{P}$$

where n_1 is the index of the lens; n_2 is the index of the cladding; P is the lens period; and f(y) represents the lens thickness as a function of y, the transverse distance from the center of the lens [2]. This system of equations can be solved for f(y), which can be directly used to generate the lens surface shape. An example Bat Ears lens train is shown in Figure 8.

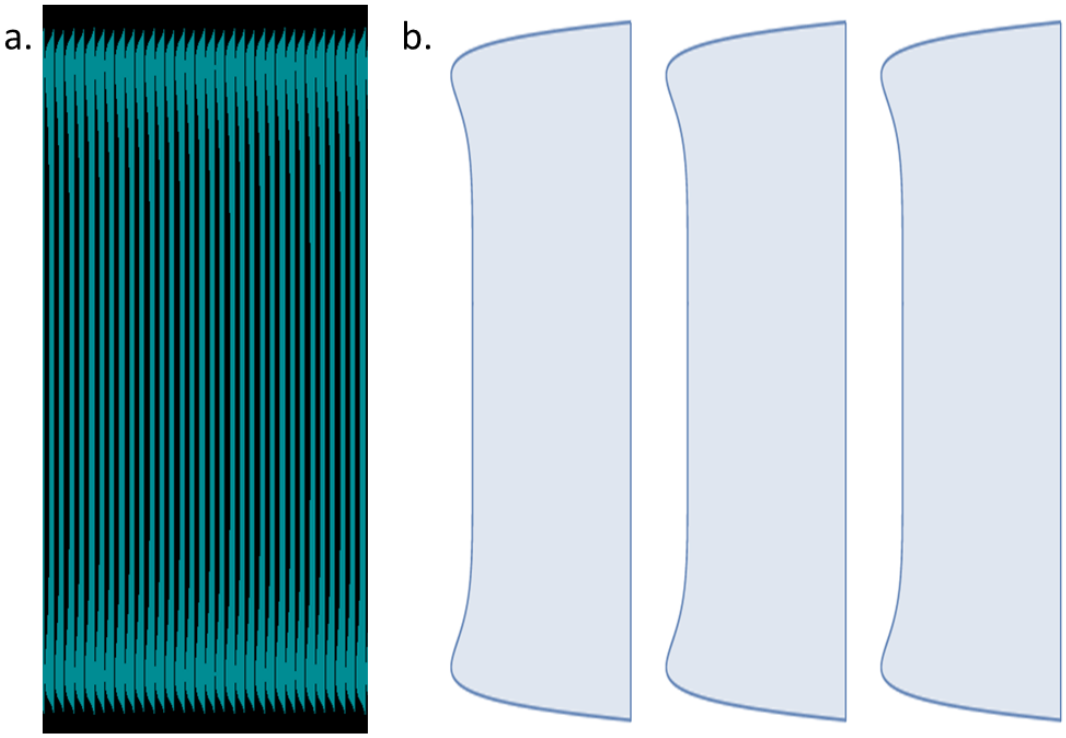

Figure 8: a) Shows a properly scaled screenshot of a Bat Ears lens train from Lumerical. b) Shows a not to scale diagram for more clarity. Note these Bat Ears lens trains are generated using a low index contrast.

The first Bat Ears train was tested using a low index contrast between the lens material and the cladding material, this was done to maximize the "lens sag" between the

peaks of the lenses and the center of the lenses, see Figure 9 for an example of lens sag. By maximizing the lens sag, the odds of being able to fabricate this device using lithography were increased, but this was found to reduce the transverse width of the lens and cause a significant amount of the supergaussian to propagate outside of the lens train structure.

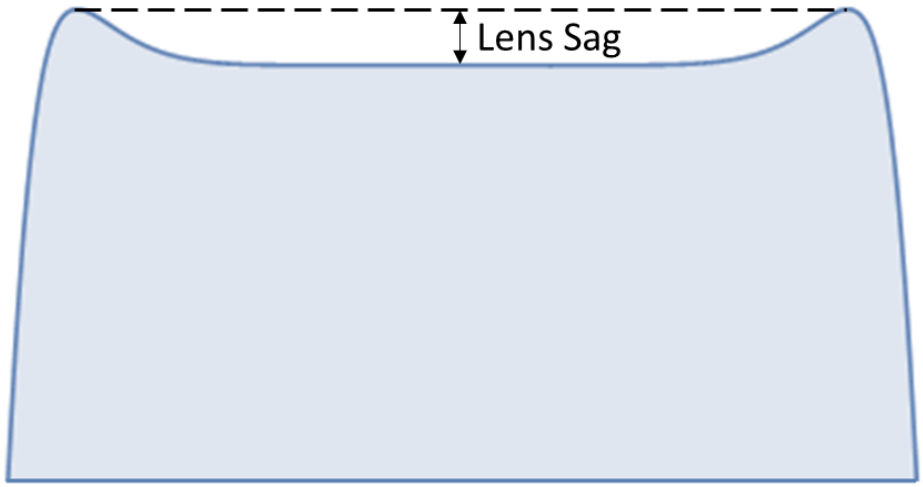

Figure 9: A diagram showcasing what is meant by lens sag. A large lens sag is desirable, as it improves the ability to accurately fabricate the lens. For a parabolic lens, the lens sag can be thought of as the lens thickness.

For testing purposes, the cladding index was decreased, increasing the index contrast and decreasing the lens sag between the thickest parts of the lenses and the center of the lenses, but also increasing the transverse width of the lenses. This was found to produce significantly better results in Lumerical. A Bat Ears lens train was designed for a 10 μm beam and beam waists of 9, 10 and 11 μm were propagated through the device to test its functionality as a waveguide, for more information, see Appendix 1. The outputs for 9 μm, 10 μm, and 11 μm beam waists are shown in Figure 10. The Strehl

ratio for the 9 μm beam was 0.9527, the Strehl ratio for the 10 μm beam was 1, and the Strehl ratio for the 11 μm beam was 0.9594.

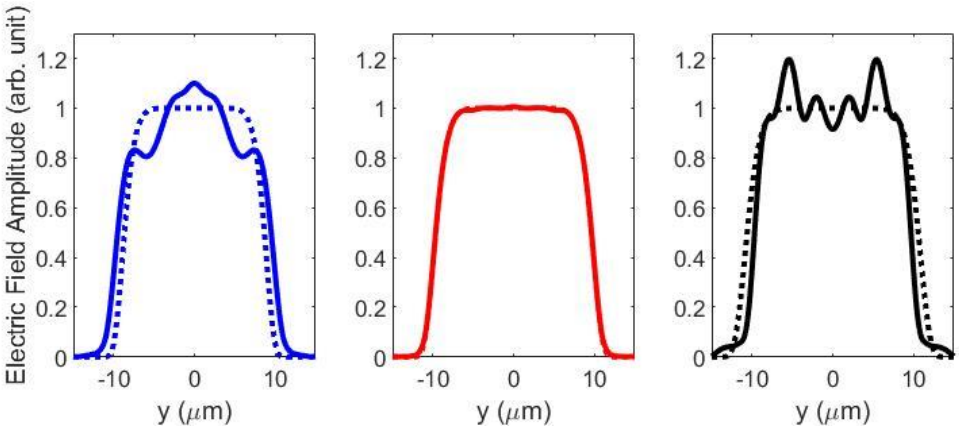

Figure 10: The output field profiles from a supergaussian beam propagating through a Bat Ears train system designed for a 10 μm beam. From left to right, the inputs to the train are a 9 μm beam, a 10 μm beam, and an 11 μm beam. The dashed lines are the input beam profiles and the solid lines are the output profiles. Note that the output profiles are scaled down to maintain conservation of energy.

With the parameters used to generate these results, the difference in lens thickness between the center of the lens and the thickest point is only 15nm, implying that the Bat Ears in this design would not be able to be reliably made using current lithographic etching techniques, and were this design etched, it would likely have a nearly uniform effective index profile and behave like a standard subwavelength waveguide without gradient index properties. To solve this problem, a new design was tested which would make the index contrast and lens sag more independent of each other.

Lens Block Lens Train

There are a few notable issues with this lens train concept. One such issue arises from the approximations used. The equations used to derive the index profiles all assume the system is in a regime where scalar wave theory holds. This puts limitations on the

size of the objects in the simulation. For example, the beam must be sufficiently large to avoid requiring vector wave theory to describe it correctly. Secondly, the index of refraction of the lenses is constrained by the geometry. Should the index of refraction be too small, the lenses can be forced to overlap, which produces an unrealizable system. The index of refraction of the lenses must also not be too large, as larger indices lead to the lens getting thinner to maintain the same effective index profile. The goal of this project is to show that 2D GRIN structures can be made with relative ease using lithography. The resolution of modern lithography is about 50nm [2], so the Bat Ears lens train discussed in the previous section cannot accurately be fabricated using modern lithography. One last issue from this design is that the difference in index of refraction between the lenses and the cladding is of vital importance to producing functional designs. Should this difference be too small, the transverse width of the lens train can become comparable to the beam waist, and a significant amount of power will be outside the guide, ruining its ability to guide the fundamental mode. Should the index contrast be too large, the lens sag can become too small to reliably make with lithography.

There are several solutions to get around the index and geometric constraint problems. The solution explored in this thesis was to substitute a percentage of the lenses with rectangular blocks, as can be shown in Figure 11.

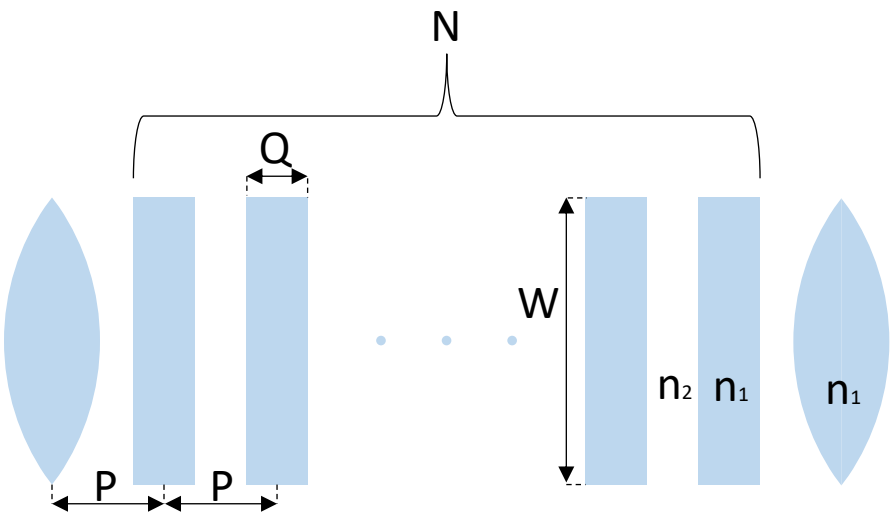

Figure 11: This image shows an example of the Lens Block Lens train and the parameters which define it. N is the number of blocks between two lenses, Q is the thickness of the blocks, P is the period between blocks and lenses, W is the transverse width of the blocks and lenses, n_1 is the index of the lenses and the blocks, n_2 is the index of the cladding. Not pictured in this diagram are the variables d and R which are used to define the lens shape and are identical to the variables d and R used in the lens train case.

This design allows for larger gaps between lenses without entering the Bragg regime, as the distance between subwavelength structures would remain the same. This would reduce the number of lenses and increase the required lensing power to maintain the same parabolic index profile, hence lenses must be thicker or have a higher index than they would in a similar parabolic lens train. The number of blocks of material between each lens can be increased or decreased, giving much more freedom to the choice in refractive indices. The issue with this design is that the effective index in a cluster of blocks will not look the same as the effective index around a lens, which should lead to some Fresnel reflection and reduced efficiency.

A Lens-Block-Lens design was generated using Mathematica. It is known from effective medium theory that the effective index for a TE mode in this structure would be

$$n_{eff}^2(y) = \frac{n_1^2\left(2\sqrt{R^2-y^2} - 2\sqrt{R^2-\left(\frac{W}{2}\right)^2} + NQ\right)}{P(N+1)} + \frac{n_2^2\left(P(N+1) - NQ - 2\sqrt{R^2-y^2} + 2\sqrt{R^2-\left(\frac{W}{2}\right)^2}\right)}{P(N+1)}$$

where N is the number of blocks between lenses and Q is the thickness of the blocks. Note that it is assumed that the blocks are the same index as the lenses, though this isn't a necessary constraint.

To test the Lens Block Lens train geometry, a structure was designed for a 4 μm beam, for more information see Appendix 1. A 2 μm beam, a 4 μm beam, and an 8 μm beam were propagated down this structure. The results from these tests showed that the Lens Block Lens train does behave like the Parabolic lens train discussed previously. The wavelength response of this system was then tested, as it was believed this would be the key difference between the devices. The transmission vs wavelength plots were generated for both the Lens train and the Lens Block Lens train and they are shown in Figure 12.

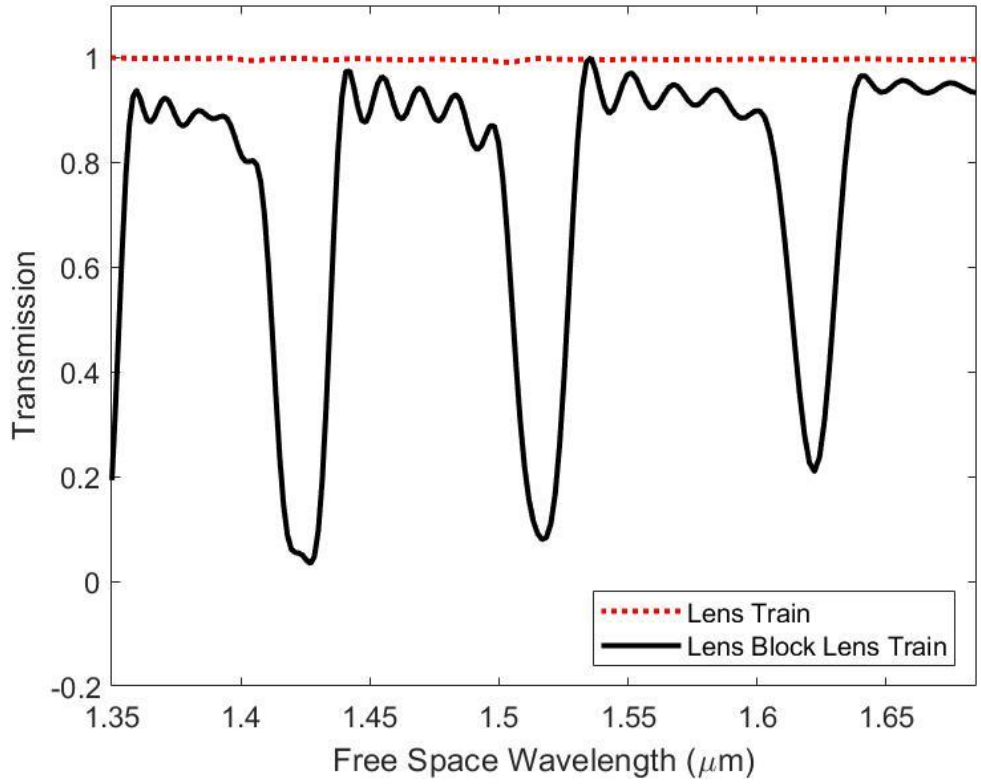

Figure 12: Transmission spectra for both the Lens train and the Lens Block Lens train generated using Lumerical's port objects. The wavelength selectivity of the Lens Block Lens train is apparent. Note that these plots were scaled to have a maximum value of 1 due to simulation errors causing the Lens Block Lens train to have transmission values over 1 and the Lens train to have about 90% transmission, much less than measured in previous tests.

From this test it is seen that the lens train has negligible frequency dependence. Should a significantly different frequency of light be used, this design would become frequency dependent, as the required lens strength is a function of the frequency, as is effective medium theory. This response is not seen here due to the narrow wavelength band tested; the largest wavelength that will experience Bragg reflection is about 1 μm. The Lens Block Lens train design did, however, have a significant transmission frequency response. The blocks between the lenses have the same effective index as the effective index at y=0 around the lenses. This means that the effective indices are well

matched at y=0, but due to the parabolic effective index around the lenses, the index matching degrades as one inspects farther away from y=0. This mismatch is enough to cause reflections to occur at every lens in the lens-block-lens train. This causes the lenses to behave like a Bragg reflector. This property is good to note as it might be useful; however, it is undesirable for this waveguide, thus this concept was not researched further.

Mode Converters

The final goal of this thesis was to develop a method of designing an arbitrary 2D GRIN profile that could be fabricated using lithography. This GRIN profile is assumed to have been generated using split step propagation and phase retrieval [7], but any method that designs an index profile would work. To accomplish this task, the GRIN profile must be converted from sampled index values to a geometric description of the lens train. There are several of ways to perform this conversion, though it decided to convert a matrix of indicies into a matrix of lens thicknesses. In this matter, any 2D index profile can be converted into a lens train.

To prove the validity of the idea, converters to convert gaussian beams with some beam waist W to tenth order supergaussian beams of the same beam waist W were designed. An example image of the geometry implemented in Lumerical is shown in Figure 13. Note that this is a subwavelength metamaterial composed of 1,000 individual lenses, not a continuous GRIN block.

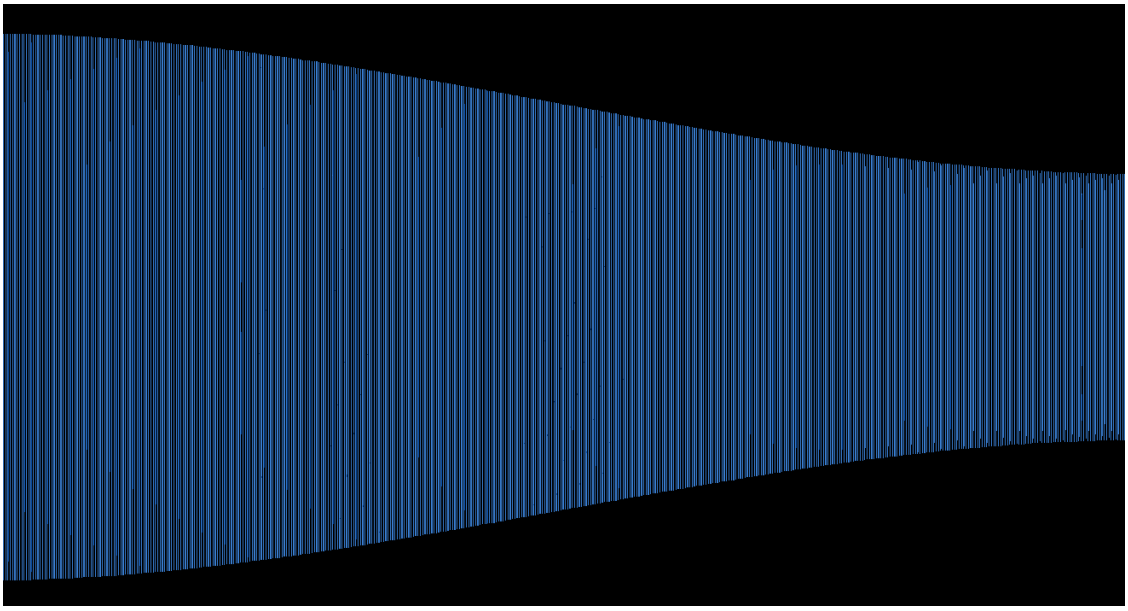

Figure 13: Shows a screenshot of a mode converter in Lumerical's simulation environment. This mode converter is for a 10 μm 10th order supergaussian beam converting to a 10 μm gaussian beam after 100 μm. It was designed to be made in silicon for a 1.5 μm beam with a glass cladding.

The lens train was designed such that it would imitate a real silicon structure. The index of the lenses was 3.47, which is the index of refraction of silicon for 1.5 μm light. The index for the cladding was set to 1.5, which is typical of glass and plastic. The gaps between lenses was at minimum 50 nm, the current lithographic limit to resolution [2]. Structures similar to the one shown were designed for beam sizes of 5 μm,10 μm, and 20 μm, as well as for device lengths of 50 μm and 100 μm, see Appendix 2 for more details. The outputs from these converters can be seen in Figure 14. The Strehl ratio and efficiency are given in Figure 14 as well. As a note, the 50 μm long converter designed to convert a 20 μm beam required more lensing power than was available, causing the width of many of the lenses to smaller than expected, reducing the performance of the device. This issue could possibly be corrected by decreasing the cladding index or allowing the gaps between lenses to be smaller than 50nm.

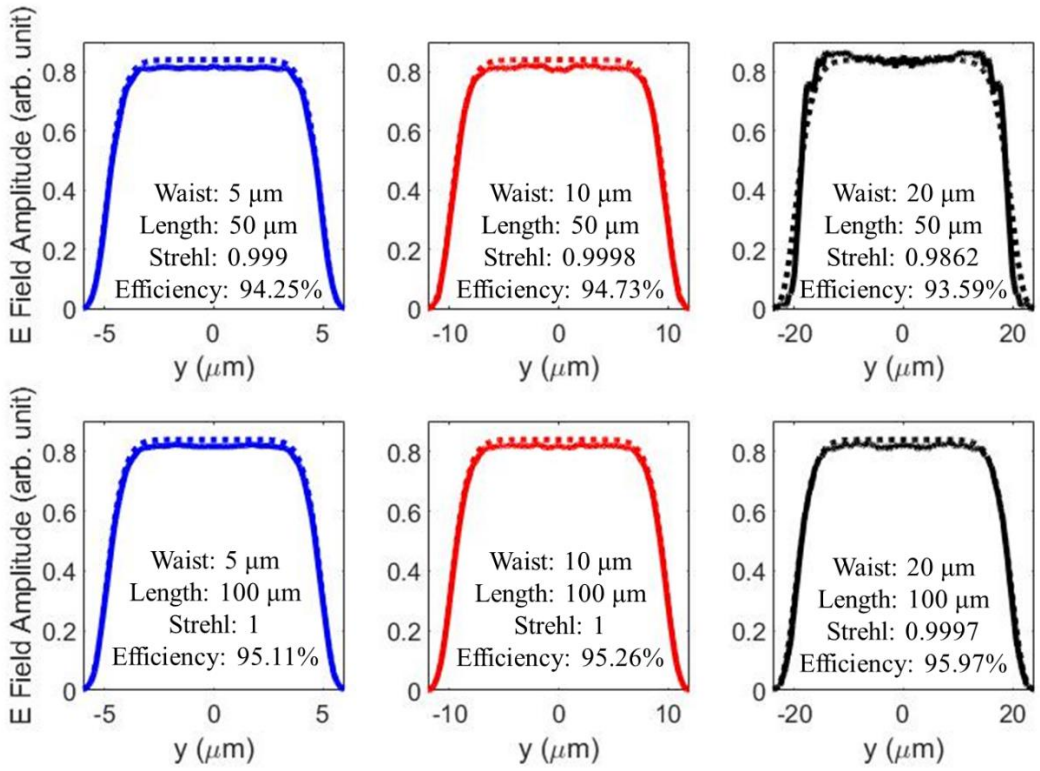

Figure 14: These are the output electric field magnitude profiles of mode converters designed to convert from gaussians to 10th order supergaussians. From left to right the beam waist increases from 5 µm to 10 µm then to 20 µm. The top row is the output from a 50 µm long converter and the bottom row is the output from a 100 µm long converter. The ideal outputs are shown by dotted lines while the experimental outputs are shown by solid lines. The Strehl ratio is given for each of the output beams, as well as the efficiency. The efficiency is the percent of input power transmitted through the converter.

As is shown by these output images, the converters can convert from a gaussian beam to a supergaussian beam with high Strehl ratio and efficiency, though there is some high spatial frequency noise in the output beam. There are several possible sources of this noise such as the finite size of each lens, the small corners on each lens due to the lenses being under sampled in the transverse direction, or possibly due to slight simulation errors due to the discrete nature of Lumerical. Approximately 95% of the power is received by the output. We believe that most of the lost power is due to back reflections in the converter. These back reflections are likely caused by lens thickness

variations in the propagation direction, as these back reflections were not present in the subwavelength waveguides. The 100 μm long devices are about 1% more efficient than their 50 μm counterparts, supporting the idea that thickness variations cause the back reflection; as a shorter converter length forces the lens thickness to make the same gradient with fewer lenses.

Using this methodology, it is possible to generate any GRIN profile using subwavelength lens-like devices in Lumerical. Unfortunately, generating these structures using modern lithographic techniques would be quite difficult. The lens thickness variations on these mode converters have been on the order of nanometers for most of the lens train, and the order of microns near the edges of the transverse direction of the lenses. This is due to the small index variation needed to focus the light properly near the center of the device, but large index variations are needed near the edges of the device to pull the long tails of the gaussian beam inward. Decreasing index contrast, or increasing the cladding material's index, allows for larger lens sag, but this decreases the transverse width of the lens, which distorts the output beam. There is perhaps a design which would correctly perform the mode conversion and can be fabricated using modern lithographic means, but this has not been explored. The Lens Block Lens train idea could also be extended to the mode converter design, but this was not explored.

Another limit to this technique is that it is expected to break down in certain size regimes. The method used to generate the GRIN profile was designed for paraxial beams, implying that beams with narrow waists relative to the wavelength will not propagate as expected through the structure. As the device length gets shorter, the design should also start to fail due to the approximations used in the split step propagator and

phase retrieval system being invalidated, this problem could likely be solved by using a ray-based approach [6]. The ray-based approach is more accurate for short device lengths than the scalar wave-based approach used to generate the mode converters in this thesis. This is because the effects of diffraction become negligible for shorter devices and the approximations used for the scalar wave-based approach start to break down, reducing the accuracy of scalar wave-based designs for short device lengths. The limits to this design process have not been thoroughly explored, and there is still much to learn about them.

Conclusion

We found a method of producing a 2D GRIN device using subwavelength lens like structures. We started by testing a set of continuous GRIN structures designed to maintain the input beam profile. These devices were found to perfectly confine and propagate the input beams. We then converted these 2D GRIN structures into subwavelength lens trains. These lens trains were designed to leverage effective medium theory to behave like a continuous GRIN device. These devices were found to work just as well as the continuous structures, but complex index profiles were found to be difficult if not impossible to fabricate with current lithographic technology. We introduced an idea for making the fabrication process easier. We then showed that 2D GRIN mode converters could be made using these subwavelength lens trains as well. These mode converters were tested and found to work remarkably well with an average Strehl ratio of 0.997 and an average transmission of 94.8%.

There are still many opportunities to learn more about these structures. The Lens Block Lens train concept was introduced, but not thoroughly investigated as a method for increasing the sag of the lens trains. This concept could be explored further as a potential method of fabricating more complex lens trains like the Bat Ears train. The mode converter design process was also introduced in this thesis, but the limitations to these devices were not explored. Neither a lower bound for the device length nor a lower bound for the device width where the converter stopped functioning well were found in this thesis, though these limitations were not sought after. Other designs that would make these converters easier to fabricate were also not explored.

Appendix 1: Subwavelength GRIN Guides

The Parabolic lens train system was designed for a lens index n_1 of 1.6, a cladding index n_2 of 1, a beam waist of 4 μm, 1.5 μm light, a background index of 1.5, and a lens period of 0.3 μm. This was implemented in Lumerical, and the results showed that the gaussian beam shape was well maintained as it propagated through the structure. The next experiment designed to test how beams of different waist sizes would propagate through the GRIN optic was performed with this same lens train.

The parameters were reworked for a lens train with lens period of 0.5 μm. We wanted to perform this test to verify that this geometry would result in a large amount of back-reflection, as the effective wavelength of 1 μm was twice the lens period, this train should be in the Bragg regime, and should experience significant back-reflection. The experiment was successful, as Lumerical predicted that this geometry would produce a trail of light as it propagated through the structure. This trail of light is exactly what is predicted for the case of Bragg Reflection, and it is caused by the light constantly getting reflected and all these reflections interfering constructively.

We next generated a Bat Ears lens train with low index contrast between the lenses and the cladding. This was done to increase the sag of the lenses, making them easier to fabricate. It was found that this low index contrast ruined the performance of the lens train as the lens width was reduced too far by the raised cladding index. To generate good results with Lumerical, we decided to test how we could maximize the lens sag while maintaining a good Strehl ratio after 200 lenses with period of 0.3 μm. Numerous Bat Ears lens train geometries were generated with the goal of having a Strehl

ratio of 1 at the output of the two hundredth lens, but also using the smallest index contrast to get the largest lens sag. The lens index was picked to ensure a minimum of a 50nm gap between lens faces, and the cladding's index was varied to locate the optimal solution. The background index was 1.5, the lenses were 0.3 μm apart, and the train was designed for a supergaussian beam with M=10, W=10 μm, and wavelength of 1.5 μm. From these tests, it was found that to maintain a Strehl ratio of 1 after 200 lenses in the system described, the cladding index should remain less than 1.43. This bound to the cladding index would likely vary for different starting parameters but is a good reference for future tests.

To prove that the Bat Ears train was designed properly, a simple test was performed where a train was designed for a 10 μm beam waist, and a few different beams were propagated through the device. For this test, the Bat Ears train designed previously was used, so the train was designed for a 1.5 μm supergaussian beam with M=10 and W=10, a lens index of 1.52, a cladding index of 1.43, a target background index of 1.5, a lens period of 0.3 μm, and a total of 200 lenses.

The equation given for designing a Lens Block Lens train can be solved alongside either the parabolic index equation for a gaussian or the supergaussian index profile for M=2 to give parameters for designing the train in Lumerical. We used a cladding index n_2=1, a lens index n_1=1.5, a grating period P=0.3 μm, a block thickness Q=0.1 μm, a free space wavelength lambda=1.5 μm, a background index n_o=1.5, the number of blocks between lenses N=19, and a beam waist w_o=4 μm for our tests. This geometry has the potential to fix the lens sag problem but has not been thoroughly tested.

Appendix 2: Mode Converters

The period between lenses in Figure 13 is 0.1 μm. This small period was required, as these converters were designed with a background index of 2.67, a lens index of 3.47, and a cladding index of 1.5 such that the lens train represents a real silicon structure. The background index was chosen such that the smallest gap between lenses was 50nm, the limit on lithographic resolution, but this large background index reduced the effective wavelength of the light down to about 0.56 μm, forcing a shorter lens period to maintain effective medium theory requirements. A period of 0.1 μm was chosen to minimize the effects of Bragg reflection expected to occur at a period larger than about 0.15 μm.. Similar structures were designed for beam sizes of 5 μm,10 μm, and 20 μm, as well as for device lengths of 50 μm and 100 μm. These converters were used to generate the results shown in Figure 14.

Appendix 3: Lumerical

For validation of our ideas, we decided to perform simulations in a finite difference time domain electromagnetic simulation software named Lumerical. Lumerical gives a lot of control over the simulation, such as how the mesh is defined, the objects in the simulation, the sources in the simulation, and the outputs recorded. This makes it very useful for simulating subwavelength GRIN structures, especially optical mode converters of this type.

This appendix is intended to explain a bit more about how Lumerical works and how we used Lumerical to generate the structures and results we needed.

Continuous GRIN Blocks

Continuous GRIN profiles are easy to implement in Lumerical. There are several different object shapes in Lumerical, though we only used rectangular prisms for the continuous GRIN blocks in our simulations. These objects can have their index set to a single value; they can be a material, which references a database of material properties for different frequencies and temperatures, or the index can be set to an equation as a function of x, y, and z. We used equations to define our continuous GRIN blocks.

Custom Sources

Lumerical comes with a few built in sources such as gaussian beams, dipoles, plane waves and mode sources. Lumerical can also generate custom sources via scripting or importing. In practice, any source can be made in Lumerical, as one has complete control over the E and H fields along the x, y, and z directions in a custom source through

scripting. In our case, we used a Lumerical script to generate supergaussian beams with all the E field in the z direction and no starting H field for testing our Bat Ears index profiles.

Subwavelength Structures

There are several ways to generate subwavelength structures in Lumerical. There exists an array function which can make a periodic structure relatively fast; but for repeated testing, scripting should be used to generate subwavelength trains. To easily generate these structures, we augmented the code from a prebuilt object in Lumerical called a grating coupler, which can be found from the components tab on the ribbon. This structure is a train of rectangular prisms on a substrate, which is very similar to the lens trains we designed. We edited the script used to generate the structure to generate custom objects rather than rectangular prisms, then set the equations for the faces of the object to match an equation generated in Mathematica. This code is accessed through the structure object, but nearly identical code can be used in a Lumerical script file, which allows for less menu hopping.

Reducing the amount of menu hopping needed to perform actions in Lumerical is of key importance with subwavelength structures. There are hundreds of individual lenses with complicated features in each structure, which causes severe rendering lag. This problem is best solved by using fewer lenses in the grating, performing all actions through Lumerical's script files, or disabling the lens trains when performing tests. Disabling the lens trains allows the user to work in Lumerical much easier when the devices are being designed initially. The lens train must be reenabled before a simulation starts though, otherwise Lumerical will ignore the lens train completely.

Ports

Ports are objects which can be placed at inputs and outputs of a device which can be used to find the wavelength response of devices; we used ports to generate the transmission vs frequency spectra in Figure 12. The biggest issue with using ports is that the ports must perform their tests using a source that they generate. Using outside sources ruins the results from the ports. The ports generate sources using fundamental mode analysis, so only the fundamental modes of the index profile at the location of the port can be used as inputs to the system. Our simulations were performed in 2D on the x and y plane, where x is the direction of propagation for the light. The effective index of our subwavelength trains varied only in y, but the actual index of refraction varied in both x and y. The port can only view the index of refraction in a line parallel to the y axis. Because of this, it views the index profile as uniform if the port is located outside of a lens; or as a slab waveguide if the port is located within a lens. The fundamental mode of a slab waveguide is not the same as the fundamental mode for a Parabolic lens train, so the port would not be able to generate the correct source profile for the structure. This means that for the Parabolic lens train, we must put the first port object inside a small continuous GRIN block such that the port generates the correct mode to propagate through the lens train.

Meshing

In Lumerical, the mesh is a structure that is used to perform the calculations of how light behaves in a system. Lumerical divides up the simulation region up into a discrete grid to perform the simulation. This grid is defined by the mesh.

There are a number of different ways to approach meshing in Lumerical. The user can place mesh override regions with uniform meshing structure. This means that the dx, dy, and dz between meshing points are constant, though not necessarily equal. These mesh override regions are good for meshing regions which need very high mesh density, but mesh override regions aren't strictly needed for a simulation. Lumerical automatically generates a mesh itself. There are 3 options for Lumerical's auto generated mesh. The uniform mesh behaves the same as a mesh object, where dx, dy, and dz are uniform across the whole simulation region, though not necessarily equal. The auto non-uniform mesh generates a mesh that is not uniform using one of many methods. The generation of these meshes can be quite complex, but this is the method that was used for this thesis. The final method is to use a custom non-uniform mesh, which behaves rather like the auto non-uniform but with extra options for the user. A general rule of thumb for making a mesh is to have the mesh be twice as fine as the smallest feature in a simulation.

How Lumerical generates the final mesh structure is quite a complicated process. The first rule to know is that Lumerical will always override the default mesh with a mesh override region's mesh. This means that for complex structures where Lumerical's default mesh may not be fine enough, the override mesh should be used. Something to note is that if Lumerical's default mesh is set to uniform and there is an override mesh region in the simulation, the override will not just override the region it is in, but the whole simulation's mesh. This is done to maintain uniformity in the total mesh.

PML Reflections

The way Lumerical deals with boundary conditions is a complicated matter, but a very important one to understand for generating good results. For a dielectric waveguide like the one discussed here, one should use a PML, or perfectly matched layer, boundary condition. PML boundary conditions are used to remove light leaving the simulation region, reducing the reflection of the wave to zero. This is done by adding layers of PML to the edge of the simulation region. The first layer of PML is designated by the innermost orange rectangle in the simulation window. The outermost layer of the PML is designated by the outermost orange rectangle in the simulation window. The space between these rectangles is filled in with orange to signify that this is the PML region. There are a few different types of PML, the ones used in this thesis were the standard and the stabilized. The standard PML should be used in most scenarios, but if the structure continues outside the PML, then the stabilized PML should be used. The stabilized PML has many more layers than the standard PML does and thus increases the simulation time. Something else to note is that if the structure does extend into the PML, then the structure should extend all the way through to outside the largest orange rectangle. This is done to maximize the effectiveness of the stabilized PML layers.

One final note about PML layers is that they do not seem to function well with subwavelength lens trains. The PML layers attempt to index match the material in the simulation region to remove reflections, but for our lens train experiments, we were unable to prevent reflections from the PML layer. This is likely due to the PML layers being unable to match the effective index of the lens train. To generate results without reflections off the back surface of the PML, we extended our subwavelength structures to

be longer than necessary, then ended the simulation using the simulation timer before the backpropagating beam could pass over our output monitor.

Mode Converter

To generate the mode converter, a matrix representing a GRIN profile was imported into MATLAB. This matrix was then was converted into a matrix of lens thicknesses. Each column of the matrix, except the first column, represented a lens, and each entry in that column was the lens thickness at a point along the transverse direction. The first column in the matrix contained the transverse sample points for each entry such that the transverse size of the lens train would remain the same between Lumerical and MATLAB. This matrix is then saved as a .txt file, and Lumerical read it using a script file. This script converts each column of the matrix into a set of coordinates, which are then set as vertices for a polygon object in Lumerical.

The process for generating the effective index of discretely sampled GRIN was straightforward in concept, though convoluted in implementation. The discrete GRIN was first up sampled using bilinear interpolation to allow a whole number of matrix elements to be combined into a single lens. This up sampling was performed on the permittivity profile rather than the GRIN profile to maintain accuracy. The up sampled permittivity profile was then divided into subsets of columns, one subset per lens, and the columns of these subsets were averaged to find the effective medium permittivity at each transverse location for each lens. The effective permittivity profiles were then used with the equation for the effective medium of a TE wave to calculate the lens thickness required to generate the correct effective index given a lens index and a cladding index. This was then compiled into a matrix and sent to Lumerical to generate lenses. The

lenses were generated in Lumerical by using the lens thicknesses to generate vertices for a polygon object. This polygon object was assumed to be a good approximation for a smooth surface for enough samples in the transverse direction of the lenses, though this may be the cause of the high frequency noise seen in our mode converter output profiles.

Bibliography

[1] D. T. Moore, "Gradient-Index Optics: A Review," *Applied Optics*, vol. 19, no. 7, pp. 1035–1038, Apr. 1980.

[2] P. Cheben, R. Halir, J. H. Schmid, H. A. Atwater, and D. R. Smith, "Subwavelength integrated photonics," *Nature*, vol. 560, no. 7720, pp. 565–572, Aug. 2018

[3] J. R. Leger, W. M. Kunkel, A. Ghoreyshi, G. Douglass, S. Gross, and M. J. Withford, "Gradient-index beam shapers: fabricated devices and 3D design," *Laser Resonators, Microresonators, and Beam Control XX*, Feb. 2018.

[4] U. Levy, M. Nezhad, H.-C. Kim, C.-H. Tsai, L. Pang, and Y. Fainman, "Implementation of a graded-index medium by use of subwavelength structures with graded fill factor," *Journal of the Optical Society of America A*, vol. 22, no. 4, pp. 724–733, Apr. 2005.

[5] A. C. Urness, M. C. Cole, and R. R. Mcleod, "Liquid deposition photolithography for the fabrication of gradient index (GRIN) micro-optics,"*Proc. SPIE 8974, Advanced Fabrication Technologies for Micro/Nano Optics and Photonics VII*, vol. 897402, Mar. 2014.

[6] D. Lin and J. R. Leger, "Numerical gradient-index design for coherent mode conversion," *Advanced Optical Technologies*, vol. 1, no. 3, pp. 195–202, July. 2012.

[7] W. M. Kunkel and J. R. Leger, "Gradient-index design for mode conversion of diffracting beams," *Optics Express*, vol. 24, no. 12, pp. 13480–13488, Jun. 2016.

[8] J. H. Schmid, P. Cheben, P. J. Bock, J. Lapointe, S. Janz, A. Delage, A. Densmore, T. J. Hall, B. Lamontagne, R. Ma, and D.-X. Xu, "Refractive index engineering with subwavelength gratings in silicon microphotonic waveguides," *IEEE Photonics Journal*, vol. 3, no. 3, pp. 597–607, Jun. 2011.

[9] U. Levy, M. Abashin, K. Ikeda, A. Krishnamoorthy, J. Cunningham, and Y. Fainman, "Inhomogenous Dielectric Metamaterials with Space-Variant Polarizability," *Physical Review Letters*, vol. 98, no. 24, Jun. 2007.

[10] J. Valentine, J. Li, T. Zentgraf, G. Bartal, and X. Zhang, "An optical cloak made of dielectrics," *Nature Materials*, vol. 8, no. 7, pp. 568–571, Apr. 2009.

[11] A. Yariv and P Yeh, "Rays and Optical Beams," in Photonics: Optical Electronics in Modern Communications, 6th ed. New York, New York, United States of America: Oxford University Press, 2007, ch. 2, pp. 66–106.

[12] T.-C. Poon and T. Kim, "Beam Propagation in Inhomogenous Media," in Engineering Optics with MATLAB, 1st ed. Singapore, Singapore: World Scientific Publishing, 2006, ch. 3, sec. 3, pp. 119–121.